48. Resonances

Updated 2017 by D.M. Asner (Brookhaven National Laboratory), C. Hanhart (Forschungszentrum Jülich) and E. Klempt (Bonn).

48.1. General Considerations

Perturbative methods can be applied to systems of quarks and gluons only for large momentum transfers (see review on 'Quantum chromodynamics') and, under certain conditions, to some properties of systems that contain heavy quarks (see review on 'Heavy-Quark and Soft-Collinear Effective Theory'). In general, however, dealing with QCD in the low momentum transfer region is a very complicated, non–perturbative problem where quarks and gluons are confined within color neutral hadrons. Physical states show up as poles of the S–matrix either on the physical sheet (bound states) or on the unphysical sheets (resonances) and manifest themselves as structures in experimental observables.

Resonances can show up either in so–called formation experiments, typically of the kind

$$A + B \to R \to C_1 + ... + C_n \ ,$$

where they become visible in an energy scan (a perfect example of this being the R–function measured in e^+e^- annihilations — *cf.* the corresponding plots in the review on 'Plots of Cross sections and related quantities'), or together with a spectator particle S in production experiments of the kind

$$A \to R + S \to [C_1 + ... + C_n] + S \ .$$

In the latter case the resonances properties are commonly extracted from a Dalitz plot analysis (see review on 'Kinematics') or projections thereof. Multi–particle final states are often parametrized in terms of successive decays of two–body resonances.

Resonance phenomena are very rich: while typical hadronic widths are of the order of 100 MeV (e.g., for the meson resonances $\rho(770)$ or $\psi(4040)$ or the baryon resonance $\Delta(1232)$) corresponding to a life time of 10^{-23} s, the widths can also be as small as sub MeV (e.g. of $X(3872)$) or as large as several hundred MeV (e.g. of the meson resonances $f_0(500)$ or $D_1(2430)$ or the baryon resonance $N(2190)$).

Ideally a resonance appears as a peak in the total cross section. If the structure is narrow and if there are no relevant thresholds or other resonances nearby, the resonance properties may be extracted employing a standard Breit-Wigner parametrization if necessary improved by using an energy dependent width term (*cf.* Sec. 2.1 of this review). However, in general, unitarity and analyticity call for the use of more refined tools. When there are overlapping resonances with the same quantum numbers, the resonance terms should not simply be added but combined in a non–trivial way either in a K–matrix approximation (*cf.* Sec. 2.3 of this review) or using more refined methods (*cf.* Sec. 1.4 of this review). Only then the proper pole parameters can be extracted that are universal resonance properties — on the contrary, Breit–Wigner parameters are typically reaction dependent. In addition, for broad resonances there is no direct relation anymore

between pole location and the total width/life time — then the pole residues need to be used in order to quantify the decay properties of a given state (*cf.* Sec. 3 of this review).

For simplicity, throughout this review the formulas are given for distinguishable, scalar particles. The additional complications that appear in the presence of spins can be controlled in the helicity framework developed by Jacob and Wick [1], or in a non-relativistic [2] or relativistic [3] tensor operator formalism. Within these frames, sequential (cascade) decays are commonly treated as a coherent sum of two-body interactions. Therefore below most explicit expressions are given for two–body kinematics.

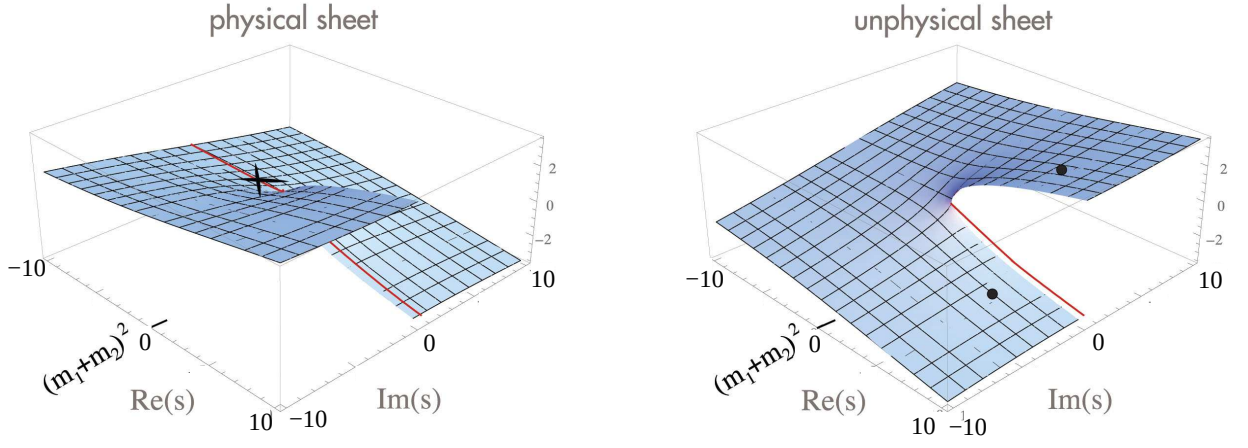

Figure 48.1: Sketch of the imaginary part of a typical single–channel amplitude in the complex s-plane. The solid dots indicate allowed positions for resonance poles, the cross for a bound state. The solid line is the physical axis (shifted by $i\epsilon$ into the physical sheet). The two sheets are connected smoothly along their discontinuities.

48.1.1. *Properties of the S-matrix* :

The unitary operator that connects asymptotic *in* and *out* states is called the S–matrix. It is an analytic function in the Mandelstam plane up to its branch points and poles. Branch points appear whenever there is a channel opening — at each threshold for massive particles the number of Riemann sheets doubles. Poles refer either to bound states or to resonances. The former poles are located on the physical sheet, the latter are located on the unphysical sheet closest to the physical one, often called the second sheet; each can be accompanied by mirror poles. If there are resonances in subsystems of multi–particle states, branch points appear in the complex plane of the unphysical sheet(s). Any of these singularities leads to some structure in the observables (see also Ref. [4]). In a partial wave decomposed amplitude additional singularities not related to resonance physics may emerge as a result of the partial-wave projection. For a discussion see, e.g., Ref. [5].

For simplicity we now restrict ourselves to reactions involving four particles. Then the kinematics of the reaction is fully described by the Mandelstam variables s, t and u, only two of them being independent (cf. Eqs. (28)-(31) of the kinematics review). Bound state poles are allowed only on the real s–axis below the lowest threshold. There

is no restriction for the location of poles on the unphysical sheets. Analyticity requires, however, that, if there is a pole at some complex value of s, there must be another pole at its complex conjugate value, s^*. The pole with a negative imaginary part is closer to the physical axis and thus influences the observables in the vicinity of the resonance region more strongly, however, at the threshold both poles are always equally important. This is illustrated in Fig. 48.1.

The S-matrix is related to the scattering matrix $\mathscr{M}$ (c.f. Eq. (8) of the kinematics review). For two–body scattering it can be cast into the form

$$S_{ab} = I_{ab} - 2i\sqrt{\rho_a}\mathscr{M}_{ab}\sqrt{\rho_b}\,. \tag{48.1}$$

$\mathscr{M}$ is a matrix in channel space and depends, for two–body scattering, on both s and t. The channel indices a and b are multi–indices specifying all properties of the channel including the conserved quantum numbers. The two-body phase-space ρ is given (cf. Eq. 12 of the kinematics review) by

$$\rho_a(s) = \frac{1}{16\pi}\frac{2|\vec{q}_a|}{\sqrt{s}}\,. \tag{48.2}$$

with q_a denoting the relative momentum of the decay particles of channel a, with masses m_1 and m_2, cf. Eq. (20a) of the kinematics review.

As discussed below, unitarity puts strong constraints on the scattering matrix. Further constraints come, e.g., from crossing symmetry and duality [6].

48.1.2. *Consequences from unitarity* :

In what follows, scattering amplitudes $\mathscr{M}$ and decay amplitudes $\mathcal{A}$ will be distinguished, since unitarity puts different constraints on these. The discontinuity of the scattering amplitude from channel a to channel b [7] is constrained by unitarity to

$$i\,[\mathscr{M}_{ba} - \mathscr{M}^*_{ab}] = (2\pi)^4 \sum_c \int d\Phi_c \mathscr{M}^*_{cb}\mathscr{M}_{ca}\,. \tag{48.3}$$

Using $\mathrm{Disc}(\mathscr{M}(s)) = 2i\,\mathrm{Im}(\mathscr{M}(s+i\epsilon))$ the optical theorem follows

$$\mathrm{Im}\,(\mathscr{M}_{aa}|_{\mathrm{forward}}) = 2q_a\sqrt{s}\,\sigma_{\mathrm{tot}}(a \to \mathrm{anything})\,. \tag{48.4}$$

The unitarity relation for a decay amplitude of a heavy state H into a channel a is given by

$$i\left[\mathcal{A}^H_a - \mathcal{A}^{H\,*}_a\right] = (2\pi)^4 \sum_c \int d\Phi_c \mathscr{M}^*_{ca}\mathcal{A}^H_c\,. \tag{48.5}$$

From Eq. (48.5) Watson's theorem follows straightforwardly: the phase of $\mathcal{A}$ agrees with that of $\mathscr{M}$ as long as only a single channel contributes. For systems where the phase shifts are known like $\pi\pi$ in S– and P–waves for low energies, $\mathcal{A}^H$ can be calculated in a model-independent way using dispersion theory [8]. Those methods can also be generalized to three–body final states [9] and were applied to $\eta \to \pi\pi\pi$ in Refs. [10,11,12] and to ϕ and ω to 3π in Ref. [13].

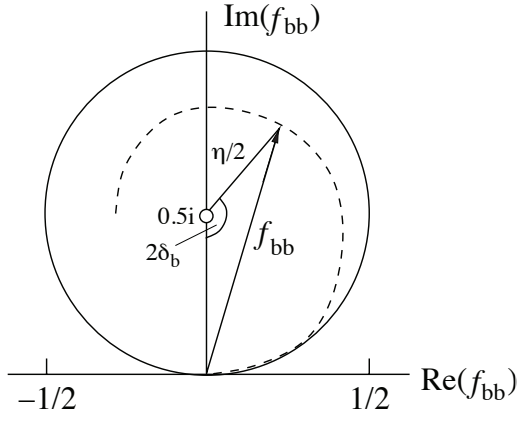

Figure 48.2: Argand plot showing a diagonal element of a partial-wave amplitude, a_{bb}, as a function of energy. The amplitude leaves the unitary circle (solid line) as soon as inelasticity sets in, $\eta < 1$ (dashed line).

48.1.3. ***Partial-wave decomposition*** :

In general, a physical amplitude $\mathscr{M}$ (c.f. Eq. (8) of the kinematics review) is a matrix in channel space. It depends, for two–body scattering, on both s and t. It is often convenient to expand the amplitudes in partial waves. For this purpose one defines for the transition matrix from channel a to channel b

$$\mathscr{M}_{ba}(s,t) = \sum_{L=0}^{\infty} (2L+1) \mathscr{M}^L_{ba}(s) P_L(\cos(\theta)) \ , \tag{48.6}$$

where L denotes the angular momentum—in the presence of spins the initial and final value of L does not need to be equal. To simplify notations below we will drop the label L. The function $\mathscr{M}_{ba}(s)$ is expressed in terms of the partial-wave amplitudes $f_{ba}(s)$ via

$$\mathscr{M}_{ba}(s) = -f_{ba}(s)/\sqrt{\rho_a \rho_b} \ . \tag{48.7}$$

The partial-wave amplitudes f_{ba} depend on s only. Using $S_{ba} = \delta_{ba} + 2i f_{ba}$ one gets from the unitarity of the S-matrix

$$f_{bb} = (\eta \exp(2i\delta_b) - 1)/2i \ , \tag{48.8}$$

where δ_b (η) denotes the phase shift (elasticity parameter — also called inelasticity) for the scattering from channel b to channel b. One has $0 \leq \eta \leq 1$, where $\eta = 1$ refers to purely elastic scattering. The evolution with energy of a partial-wave amplitude f_{bb} can be displayed as a trajectory in an Argand plot, as shown in Fig. 48.2. In case of a two–channel problem the off–diagonal element is typically parametrized as $f_{ba} = \sqrt{1-\eta^2}/2 \, \exp(i(\delta_b + \delta_a))$.

48.1.4. ***Explicit parametrizations for scattering and production amplitudes*** :

It is often convenient to decompose the physical amplitude $\mathscr{M}$ into a pole part and a non–pole part, often called background

$$\mathscr{M} = \mathscr{M}^{\text{b.g.}} + \mathscr{M}^{\text{pole}} \ . \tag{48.9}$$

The splitting given in Eq. (48.9) is reaction dependent and not unique (see, e.g., the discussion in Ref. [14]) , such that some resonances show up differently in different reactions. Independent of the reaction are, however, the location of the pole of a given resonance R in the complex s-plane, s_{R}, and its residues, or, more accurately, the pole couplings introduced in the last section of this review. Those parameters capture all the properties of a given resonance. The decomposition of Eq. (48.9) is employed, e.g., in Ref. [15] to study the lineshape of $\psi(3770)$ and in Refs. [16,17] to investigate πN scattering. Traditionally one introduces the notation

$$\sqrt{s_{\text{R}}} = M_{\text{R}} - i\Gamma_{\text{R}}/2 \ , \tag{48.10}$$

where M_{R} and Γ_{R} are referred to as mass and total width of the resonance R, respectively. Note, the standard Breit-Wigner parameters M_{BW} and Γ_{BW}, also introduced below, in general deviate from the pole parameters, e.g., due to finite width effects and the influence of thresholds.

If there are N resonances in a particular channel,

$$\mathscr{M}^{\text{pole}}_{ba}(s) = \gamma_b(s)[1 - V^{\text{R}}(s)\Sigma(s)]^{-1}_{bc} V^{\text{R}}_{ca}(s)\gamma_a(s) \ . \tag{48.11}$$

where all ingredients are matrices in channel space. Especially

$$V^{\text{R}}_{ab}(s) = -\sum_{n=1}^{N} \frac{g_{n\,b}\ g_{n\,a}}{s - M_n^2} \ , \tag{48.12}$$

γ_a and Σ_a denote the normalized vertex function and the self-energy, respectively, while $g_{n\,a}$ denotes the coupling of the resonance R_n to channel a and M_n its mass parameter (not to be confused with the pole position). The sign in Eq. (48.12) is necessary to render the g–parameters real. A relation analogous to Eq. (48.5) holds for any kind of production amplitude — especially for the normalized vertex functions, however, with the final state interaction provided by $\mathscr{M}^{\text{b.g.}}$

$$i\,[\gamma_a - \gamma_a^*] = (2\pi)^4 \sum_c d\Phi_c \left(\mathscr{M}^{\text{b.g.}}\right)^*_{ca} \gamma_c \ . \tag{48.13}$$

The discontinuity of the self-energy $\Sigma_a(s)$ is

$$i\,[\Sigma_a - \Sigma_a^*] = (2\pi)^4 \int d\Phi_a |\gamma_a|^2 \ . \tag{48.14}$$

The real part of Σ_a can be calculated from Eq. (48.14) via a properly subtracted dispersion integral. If $\mathscr{M}^{\text{b.g.}}$ is unitary, the use of Eq. (48.11) leads to a unitary full amplitude, cf. Eq. (48.9).

For a single resonance ($N = 1$) Eq. (48.11) reads

$$\mathscr{M}_{\text{pole}}(s)_{ba}\big|_{N=1} = -\gamma_b(s)\frac{g_b\ g_a}{s - \hat{M}_{\text{R}}(s)^2 + i\sqrt{s}\Gamma^{\text{R}}(s)_{\text{tot}}}\gamma_a(s)\ , \tag{48.15}$$

where the mass function $\hat{M}_{\text{R}}(s)^2 = M^2 + \sum_c g_c^2 \text{Re}(\Sigma_c)$. The imaginary part of the self-energy gives the width of the resonance via

$$\Gamma_c^{\text{R}}(s) = \frac{(2\pi)^4}{2\sqrt{s}} g_c^2 \int d\Phi_c |\gamma_c|^2;\ \Gamma^{\text{R}}(s)_{\text{tot}} = \sum_c \Gamma_c^{\text{R}}(s)\ . \tag{48.16}$$

Here the sum runs over all channels. Eq. (48.16) agrees with Eq. (10) of the kinematics review.

In the absence of left–hand cuts in the production mechanism, the decay amplitude of some heavy state H can be written as

$$\mathcal{A}_a^H(s) = \gamma_a(s)\left[1 - V^{\text{R}}(s)\Sigma(s)\right]^{-1}_{ab}\mathcal{P}_b^H(s)\ , \tag{48.17}$$

where $\mathcal{P}^H$ is a vector in channel space that may be parametrized as

$$\mathcal{P}_b^H(s) = p_b(s) - \sum_{n=1}^{N}\frac{g_{n\,b}\ \alpha_n^H}{s - M_n^2} \tag{48.18}$$

and the masses M_n need to agree with those in V_{R}. The function $p_a(s)$ is a background term and the α_n^H denote the coupling of the heavy state H to the particular resonance R_n. If there are additional particles in the final state of the studied decay of the heavy state H, not included in the non-perturbative treatment of Eq. (48.17), then they also contain the corresponding kinematic factors related to their coupling. If these additional particles are interacting strongly, a complete few–body treatment of the final state becomes necessary, especially since rescattering effects can introduce additional complex phases [18]. However, in practice those effects as well as those from missing channels are often parametrized by choosing the parameters α_n^H complex valued. With some additional assumptions, Eq. (48.9) and Eq. (48.17) were employed in Ref. [19] to study the pion vector form factor. An alternative parametrization for the production amplitude that is convenient, if the full matrix $\mathscr{M}$ — including the resonances — is known, cf. Ref. [20]

$$\mathcal{A}_a^H(s) = \mathscr{M}_{ab}(s)\tilde{\mathcal{P}}_b^H(s)\ . \tag{48.19}$$

The function $\tilde{\mathcal{P}}_H(s)_b$ needs to cancel the left–hand cuts of $\mathscr{M}$ and therefore could be strongly energy dependent. In actual applications a low-order polynomial turned out to

be sufficient — c.f. Ref. [21,22] for a study of $\gamma\gamma \to \pi\pi$. As above, to preserve unitarity the coefficients of $\tilde{\mathcal{P}}_H(s)_b$ need to be real, however, in practice rescattering effects or missing channels are parametrized by complex valued parameters.

Three-body decays are often represented by Dalitz plots. It is often of interest to quantify the contribution of a single amplitude $\mathcal{A}_a^H$ to the decay of a heavy resonance H, where now $\mathcal{A}_a^H$ needs to be generalized to three body kinematics either completely by considering the full three–body final state interactions or effectively by choosing complex vertex parameters. Then fractional contributions are introduced (since different intermediate states leading to the same final state interfere, the assignment of branching ratios is to be taken with some caution) via

$$\mathrm{F}_a^H = \frac{\int d\Phi |\mathcal{A}_a^H|^2}{\int d\Phi |\sum_a \mathcal{A}_a^H|^2} \tag{48.20}$$

where the phase space integral $d\Phi$ extends over the Dalitz plot region and the angular dependence of the subsystems needs to be kept (cf. Eq. (48.6)). Typically the effect of interference terms in the denominator is small.

The formulas given so far are completely general. However, they require as input, e.g., information on all relevant channels. It is therefore often necessary and appropriate to find approximations/parameterizations.

48.2. Common parameterizations for resonances

In most common parameterizations the non–pole interaction, $\mathscr{M}^{\mathrm{b.g.}}$, is omitted. While this is a bad approximation for, e.g., scalar–isoscalar $\pi\pi$ interactions at very low energies [23], under more favorable conditions this can be justified. Thus in what follows we will assume $\mathscr{M}^{\mathrm{b.g.}} = 0$, which leads to real vertex functions. For two–body channels one writes

$$\gamma(s)_a = q_a^{L_a} F_{L_a}(q_a, q_\mathrm{o}) \ ,$$

where L_a denotes the angular momentum of the decay products, giving rise to the centrifugal barrier $q_a^{L_a}$, where q_a denotes the relative momentum of the outgoing particle pair defined in the rest frame of the decaying particle, cf. Eq. (20a) of the kinematics review. Often one introduces a phenomenological form factor, here denoted by $F_{L_a}(q_a, q_\mathrm{o})$. It depends on the channel momentum as well as some intrinsic scale q_o. Often the Blatt-Weisskopf form is chosen [24,25], where, e.g., $F_0^2 = 1$, $F_1^2 = 2/(q_a + q_\mathrm{o})$ and $F_2^2 = 13/((q_a - 3q_\mathrm{o})^2 + 9q_a q_\mathrm{o})$. In addition, for isolated, narrow resonances the couplings g_a can be related to the partial widths, $\Gamma_{\mathrm{R}\to a}$, via

$$g_a = \frac{1}{\gamma_a(s_\mathrm{R})} \sqrt{\frac{M_\mathrm{R}\Gamma_{\mathrm{R}\to a}}{\rho_a}} \ , \tag{48.21}$$

where M_R was defined in Eq. (48.10).

48.2.1. ***The Breit–Wigner and Flatté Parametrizations*** :

If there is only a single resonance present and all relevant thresholds are far away, then one may replace $\Gamma_{\rm R}(s)_{\rm tot}$ with a constant, $\Gamma_{\rm BW}$. Under these conditions also the real part of Σ is a constant that can be absorbed into the mass parameter and Eq. (48.15) simplifies to

$$\mathscr{M}_{ba}^{\rm pole}\Big|_{N=1} = -\frac{g_b\ g_a}{s - M_{\rm BW}^2 + i\sqrt{s}\Gamma_{\rm BW}}\ , \tag{48.22}$$

which is the standard Breit–Wigner parametrization. For a narrow resonance it is common to replace $\sqrt{s}$ by $M_{\rm BW}$. If there are nearby relevant thresholds, $\Gamma_{\rm BW}$ needs to be replaced by $\Gamma(s)$. For two–body decays one writes

$$\Gamma(s) = \sum_c \Gamma_{{\rm R}\to c}\left(\frac{q_c}{q_{{\rm R}\,c}}\right)^{2L_c+1}\left(\frac{M_R}{\sqrt{s}}\right)\left(\frac{F_{L_c}(q_c,q_{\rm o})}{F_{L_c}(q_{{\rm R}\,c},q_{\rm o})}\right)^2\ , \tag{48.23}$$

where $q_{{\rm R}\,c} = q(M_{\rm BW})_c$ denotes the decay momentum of resonance R into channel c. The Breit-Wigner parameters $M_{\rm BW}$ and $\Gamma_{\rm BW}$ agree with the pole parameters only if $M_{\rm R}\Gamma(M_{\rm R}) \ll M_{\rm thr.}^2 - M_{\rm R}^2$, with $M_{\rm thr.}$ for the closest relevant threshold. Otherwise the Breit-Wigner parameters deviate from the pole parameters and are reaction dependent.

If there is more than one resonance in one partial wave that significantly couples to the same channels, it is in general incorrect to use a sum of Breit-Wigner functions, for it may violate unitarity constraints. Then more refined methods should be used, like the K–matrix approximation described in the next section.

Below the corresponding threshold, q_c in Eq. (48.23) must be continued analytically: if, e.g., the particles in channel c have equal mass m_c, then

$$q_c = \frac{i}{2}\sqrt{4m_c^2 - s} \quad \text{for} \quad \sqrt{s} < 2m_c\ . \tag{48.24}$$

The resulting line shape above and below the threshold of channel c is called Flatté parametrization [26]. If the coupling of a resonance to the channel opening nearby is very strong, the Flatté parametrization shows a scaling invariance and does not allow for an extraction of individual partial decay widths, but only of ratios [27].

48.2.2. ***The K–matrix approximation*** :

As soon as there is more than one resonance in one channel, the use of the K–matrix approximation should be preferred compared to the Breit–Wigner parametrization discussed above. From the considerations formulated in Eq. (48.11), the K–matrix approximation follows straightforwardly by replacing the self-energy Σ_c by its imaginary part in the absence of $\mathscr{M}^{\rm b.g.}$, but keeping the full matrix structure of $V^{\rm R}$. Thus, for two–body intermediate states one writes within this scheme for the self-energy

$$\Sigma(s)_c \to i\rho_c\,\gamma(s)_c^2\ . \tag{48.25}$$

However, in distinction to the Breit-Wigner approach, $V^{\rm R}$, then called K–matrix, is kept in the form of Eq. (48.12). The decay amplitude given in Eq. (48.17) then takes the form of the standard P–vector formalism introduced in Ref. [28]. For $N = 1$ the amplitude derived from the K–matrix is identical to that of Eq. (48.22).

Some authors use the analytic continuation of ρ_c below the threshold via the analytic continuation of the particle momentum as described above [29,30].

48.2.3. ***Further improvements*** :

The K–matrix described above usually allows one to get a proper fit of physical amplitudes and it is easy to deal with, however, it also has an important deficit: it violates constraints from analyticity — e.g., ρ_a, defined in Eq. (48.2), is ill-defined at $s = 0$ and for unequal masses develops an unphysical cut. In addition, the analytic continuation of the amplitudes into the complex plane is not controlled and typically the parameters of broad resonances come out wrong (see, e.g., minireview on scalar mesons). A method to improve the analytic properties was suggested in Refs. [31–34]. It basically amounts to replacing the phase-space factor $i\rho_a$ in Eq. (48.25) by an analytic function that produces the identical imaginary part on the right-hand cut. In the simplest case of a channel with equal masses the expressions that can be used for real values of s read

$$-\frac{\hat{\rho}_a}{\pi}\log\left|\frac{1+\hat{\rho}_a}{1-\hat{\rho}_a}\right|,\ -\frac{2\hat{\rho}_a}{\pi}\arctan\left(\frac{1}{\hat{\rho}_a}\right),\ -\frac{\hat{\rho}_a}{\pi}\log\left|\frac{1+\hat{\rho}_a}{1-\hat{\rho}_a}\right|+i\hat{\rho}_a$$

for $s < 0$, $0 < s < 4m_a^2$, and $4m_a^2 < s$, respectively, with $\hat{\rho}_a = \sqrt{|1-4m_a^2/s|}$ for all values of s, extending the expression of Eq. (48.2) into the regime below threshold. The more complicated expression for the case of different masses can be found, e.g., in Ref. [32].

If there is only a single resonance in a given channel, it is possible to feed the imaginary part of the Breit-Wigner function, Eq. (48.22) with an energy-dependent width, directly into a dispersion integral to get a resonance propagator with the correct analytic structure [35,36].

48.3. Properties of resonances

A resonance is characterized not only by its complex pole position but also by its residues that quantify its couplings to the various channels and allow one to define a branching ratio also for broader resonances. In the Meson Particle Listings the two-photon width of $f_0(500)$ is defined in terms of the corresponding residue. The Baryon Particle Listings give the elastic pole residues and normalized transition residues. However, different conventions are used in the two sectors, which are shortly outlined here.

In the close vicinity of a pole the scattering matrix $\mathscr{M}$ can be written as

$$\lim_{s\to s_R}\mathscr{M}_{ba} = -\frac{\mathscr{R}_{ba}}{s-s_{\rm R}}\ , \tag{48.26}$$

where $s_{\rm R}$ denotes the pole position of the resonance R. The sign convention in Eq. (48.26) is consistent with that of Eq. (48.12). The residues may be calculated via an integration along a closed contour around the pole using

$$\mathscr{R}_{ba} = \frac{i}{2\pi}\oint ds\mathscr{M}_{ba}\ .$$

The factorization of the residue $(\mathscr{R}_{ba})^2 = \mathscr{R}_{aa}\times\mathscr{R}_{bb}$ allows one to introduce pole couplings according to

$$\tilde{g}_a = \mathscr{R}_{ba}/\sqrt{\mathscr{R}_{bb}}\ . \tag{48.27}$$

The pole couplings are the only quantities that allow one quantify the transition strength of a given resonance to some channel a independent of how the particular resonance got produced. For a single, narrow state with an energy-independent background in the resonance region, far away from all relevant thresholds one finds $\tilde{g}_a = \gamma_a(s_{\rm R})g_a$ with the real valued resonance couplings g_a defined in Eq. (48.12) accompanied by the complex valued vertex functions γ_a introduced in Eq. (48.11). Based on this observation one may use the straightforward generalization of Eq. (48.21) to define a partial width and a branching fraction even for a broad resonance via

$$\Gamma_{{\rm R}\to a} = \frac{|\tilde{g}_a|^2}{M_{\rm R}}\rho_a(M_{\rm R}^2) \quad \text{and} \quad Br_a = \Gamma_{{\rm R}\to a}/\Gamma_{\rm R} \ , \tag{48.28}$$

where $M_{\rm R}$ and $\Gamma_{\rm R}$ were introduced in Eq. (48.10). This expression was used to define a two–photon width for the broad $f_0(500)$ (also called σ) [21,22]. Eq. (48.28) defines a partial decay width independent of the reaction used to extract the parameters. It maps smoothly onto the standard definitions for narrow resonances — cf. Eq. (48.16). There are cases where a resonance couples to a channel that opens only above $M_{\rm R}$. A prominent example for this being $f_0(980)$ to $\bar{K}K$. If one wants to define a branching fraction that also captures this situation one may define

$$Br'_a = \int\limits_{\rm threshold}^{\infty} \frac{ds}{\pi}\frac{|\tilde{g}_a|^2\rho(s)}{|D(s)|^2} \ . \tag{48.29}$$

Here one needs to assume a line shape for the resonance R. A possible choice is a Flatté form

$$|D(s)|^2 = (M_{\rm R}^2 - s)^2 + (\sum_a |\tilde{g}_a|^2\rho_a(s))^2 \ . \tag{48.30}$$

If the s–dependence of the phase space factors is large (as is the case, e.g., for multi–particle final states) the spectral shape that emerges from the choice in Eq. (48.30) may deviate significantly from what one would expect from the corresponding pole in the complex plane. In those situations it might be appropriate to refine the parameters of Eq. (48.29) somewhat as was suggested, e.g., in Ref. [38]. In any case the only model-independent quantities are the pole couplings/residues — both forms, Eq. (48.28) and Eq. (48.29), are in general not directly related to observables but only meant to quantify the effect of the pole couplings by employing better known quantities.

In the baryon sector it is common to define the residue with respect to the partial-wave amplitudes $f_{ba}(s)$ defined in Eq. (48.7) and with respect to $\sqrt{s}$ instead of s. Accordingly in the baryon listings the elastic pole residue, which refers to $\pi N \to \pi N$ scattering, is related to the residues introduced above via

$$r = \frac{\rho_{\pi N}(s_{\rm R})}{\sqrt{4s_{\rm R}}}\,\mathscr{R}_{\pi N,\pi N} \ , \tag{48.31}$$

where the phase space factor is to be evaluated at the pole.

References:

1. M. Jacob and G. C. Wick, Annals Phys. **7**, 404 (1959) [Annals Phys. **281**, 774 (2000)].
2. C. Zemach, Phys. Rev. **140B**, 97, 109 (1965).
3. A. V. Anisovich *et al.*, J. Phys. G **28**, 15 (2002), Eur. Phys. J. A **24**, 111 (2005).
4. A rapid change in an amplitude is not an unambiguous signal of a singularity of the S–matrix [37], however, for realistic interactions this connection holds.
5. G. Höhler, *Pion-Nucleon Scattering – Methods and Results of Phenomenological Analyses*, Springer-Verlag Berlin, Heidelberg, New York, 1983.
6. M. Fukugita and K. Igi, Phys. Rept. **31** (1977) 237.
7. M. P. Peskin and D. V. Schroeder, *An Introduction to Quantum Field Theory*, Westview Press, 1995.
8. R. Omnes, Nuovo Cim. **8**, 316 (1958).
9. N. N. Khuri and S. B. Treiman, Phys. Rev. **119**, 1115 (1960).
10. J. Kambor, C. Wiesendanger and D. Wyler, Nucl. Phys. B **465**, 215 (1996).
11. A. V. Anisovich and H. Leutwyler, Phys. Lett. B **375**, 335 (1996).
12. S. P. Schneider, B. Kubis and C. Ditsche, JHEP **1102**, 028 (2011).
13. F. Niecknig, B. Kubis and S. P. Schneider, Eur. Phys. J. C **72**, 2014 (2012).
14. D. Djukanovic, J. Gegelia and S. Scherer, Phys. Rev. D **76** (2007) 037501.
15. N. N. Achasov and G. N. Shestakov, Phys. Rev. D **86**, 114013 (2012).
16. A. Matsuyama, T. Sato and T. -S. H. Lee, Phys. Rept. **439**, 193 (2007).
17. M. Döring et al., Phys. Lett. B **681**, 26 (2009).
18. I. Caprini, Phys. Lett. B **638**, 468 (2006).
19. C. Hanhart, Phys. Lett. B **715**, 170 (2012).
20. K. L. Au, D. Morgan and M. R. Pennington, Phys. Rev. D **35**, 1633 (1987).
21. D. Morgan and M. R. Pennington, Z. Phys. C **37** (1988) 431 [Erratum-ibid. C **39** (1988) 590].
22. D. Morgan and M. R. Pennington, Z. Phys. **C48**, 623 (1990).
23. J. Gasser and U. G. Meißner, Nucl. Phys. B **357**, 90 (1991).
24. J. Blatt and V. Weisskopf, *Theoretical Nuclear Physics*, New York: John Wiley & Sons (1952).
25. S. U. Chung *et al.*, Annalen Phys. **4**, 404 (1995).
26. S.M. Flatté, Phys. Lett. B **63**, 224 (1976).
27. V. Baru *et al.*, Eur. Phys. J. A **23**, 523 (2005).
28. I.J.R. Aitchison, Nucl. Phys. **A189**, 417 (1972).
29. J. H. Reid and N. N. Trofimenkoff, J. Math. Phys. **25**, 3540 (1984)..
30. V.V. Anisovich and A.V. Sarantsev, Eur. Phys. J. A **16**, 229 (2003).
31. M. R. Pennington, T. Mori, S. Uehara, Y. Watanabe, Eur. Phys. J. **C56**, 1 (2008).
32. J. A. Oller and E. Oset, Phys. Rev. D **60**, 074023 (1999).
33. N. N. Achasov and A. V. Kiselev, Phys. Rev. D **83**, 054008 (2011).
34. A. V. Anisovich *et al.*, Phys. Rev. D **84**, 076001 (2011).
35. E. L. Lomon and S. Pacetti, Phys. Rev. D **85**, 113004 (2012) [Erratum-ibid. D **86**, 039901 (2012)].
36. B. Moussallam, Eur. Phys. J. C **73** (2013) 2539.

37. G. Calucci, L. Fonda and G. C. Ghirardi, Phys. Rev. **166**, 1719 (1968).
38. A. V. Anisovich *et al.*, Phys. Lett. B **772** (2017) 247.